Decavanadate modulates gating of TRPM4 cation channels

Bernd Nilius, Jean Prenen, Annelies Janssens, Thomas Voets and Guy Droogmans

Department of Physiology, Campus Gasthuisberg, KU Leuven, Leuven, Belgium

We have tested the effects of decavanadate (DV), a compound known to interfere with ATP binding in ATP-dependent transport proteins, on TRPM4, a Ca^{2+}-activated, voltage-dependent monovalent cation channel, whose activity is potently blocked by intracellular ATP^{4-}. Application of micromolar Ca^{2+} concentrations to the cytoplasmic side of inside-out patches led to immediate current activation followed by rapid current decay, which can be explained by an at least 30-fold decreased apparent affinity for Ca^{2+}. Subsequent application of DV (10 μM) strongly affected the voltage-dependent gating of the channel, resulting in large sustained currents over the voltage range between −180 and +140 mV. The effect of DV was half-maximal at a concentration of 1.9 μM. The Ca^{2+}- and voltage-dependent gating of the channel was well described by a sequential kinetic scheme in which Ca^{2+} binding precedes voltage-dependent gating. The effects of DV could be explained by an action on the voltage-dependent closing step. Surprisingly, DV did not antagonize the effect of ATP^{4-} on TRPM4, but caused a nearly 10-fold increase in the sensitivity of the ATP^{4-} block. TRPM5, which is the most homologous channel to TRPM4, was not modulated by DV. The effect of DV was lost in a TRPM4 chimera in which the C-terminus was substituted with that of TRPM5. Deletion of a cluster in the C-terminus of TRPM4 containing positively charged amino acid residues with a high homology to part of the decavanadate binding site in SERCA pumps, completely abolished the DV effect but also accelerated desensitization. Deletion of a similar site in the N-terminus had no effects on DV responses. These results indicate that the C-terminus of TRPM4 is critically involved in mediating the DV effects. In conclusion, decavanadate modulates TRPM4, but not TRPM5, by inhibiting voltage-dependent closure of the channel.

(Resubmitted 29 June 2004; accepted after revision 25 August 2004; first published online 26 August 2004)
Corresponding author B. Nilius: Laboratorium voor Fysiologie, Campus Gasthuisberg, KU Leuven, Herestraat 49, B-3000 Leuven, Belgium. Email: bernd.nilius@med.kuleuven.ac.be

TRPM4 is a Ca^{2+}-activated but Ca^{2+}-impermeable monovalent cation channel belonging to the melastatin subfamily of transient receptor potential (TRP) membrane proteins (Launay *et al.* 2002). Other unique properties of TRPM4, besides its activation by Ca^{2+}, are its voltage dependence (Hofmann *et al.* 2003; Nilius *et al.* 2003) and block by ATP^{4-} (Nilius *et al.* 2004). Ca^{2+}-activated, non-selective cation channels (NSC) with properties reminiscent of TRPM4 and the homologous TRPM5 have been reported in various excitable and non-excitable cell types (Maruyama & Petersen, 1982; Suh *et al.* 1999, 2002; Koivisto *et al.* 2000; Ringer *et al.* 2000; Halonen & Nedergaard, 2002; Hurwitz *et al.* 2002; Magistretti & Alonso, 2002; Csanady & Adam-Vizi, 2003; Eto *et al.* 2003; Liman, 2003; Miyoshi *et al.* 2004; Rodighiero *et al.* 2004; Simard & Chen, 2004) exerting various cell functions, ranging from pacemaking and generation of cardiac afterdepolarizations (Guinamard *et al.* 2002, 2004), short-term memory (Egorov *et al.* 2002), vasomotor control (Suh *et al.* 2002) to volume regulation (Koch & Korbmacher, 1999) (for a review see Petersen, 2002). In particular, ATP-sensitive NSCs with an intrinsic voltage dependence and a single channel conductance of 25 pS comparable to that of TRPM4 have been observed in cardiomyocytes (Colquhoun *et al.* 1981; Guinamard *et al.* 2002, 2004; Wu, 2003; Zhainazarov, 2003.). Molecular identification of these TRPM4-like channels as well as understanding their function is hampered by the lack of selective modulating tools.

So far, TRPM4 channels have only been studied in heterologous expression systems (Launay *et al.* 2002; Nilius *et al.* 2003, 2004) but have also been identified as endogenous currents in HEK 293 cells (Launay *et al.* 2002). The functional analysis of this channel turned out to be relatively difficult because of the decay of channel activity in whole-cell and cell-free patch clamp measurements. The reason for this decay is not yet known. Very likely, the Ca^{2+} sensitivity of TRPM4 is regulated and partly or

 DOI: 10.1113/jphysiol.2004.070839

sometimes completely lost during the experiment, as has been suggested for the related TRPM5 desensitization (Liu & Liman, 2003).

This study focuses on properties of human TRPM4. In the first part, we present a quantitative approach to predict the observed changes in voltage dependence due to desensitization, indicating that Ca^{2+} and voltage sensitivity are interdependent. In the second part, we identify decavanadate (DV) as a strong modifier of TRPM4 channel gating. We were led by a recent report of Csanady & Adam-Vizi, 2004) who reported that the ATP block of Ca^{2+}-activated non-selective cation channels in brain capillary endothelium is antagonized by DV, a compound known to interact with ATP binding sites. DV contains six negative charges that induce strong electrostatic interactions with sites accumulating positive charges, such as the ATP binding sites of various ABC ATPases, e.g. SERCA pumps (Toyoshima *et al.* 2000; Clausen *et al.* 2003) or the ATP, actin and DV binding myosin head segment, subfragment 1 (Tiago *et al.* 2004). Our results indicate that in contrast to the endogenous channels in brain capillary endothelium DV does not antagonize ATP block of TRPM4, but rather acts as channel activator by inhibiting voltage-dependent closure of the channel.

Methods

Cell culture

Human embryonic kidney cells, HEK293, were grown in Dulbecco's modified Eagle's medium (DMEM) containing 10% (v/v) human serum, 2 mM L-glutamine, 2 U ml^{-1} penicillin and 2 mg ml^{-1} streptomycin at 37°C in a humidity controlled incubator with 10% CO_2.

Transient expression of hTRPM4 and mutagenesis

We used the recombinant bicistronic expression plasmid pdiTRPM4b, which carries the entire protein-coding region for the human TRPM4b (accession number AX443227) (Nilius *et al.* 2003) or mouse TRPM5 (accession number AY280364) (Perez *et al.* 2002) and for the green fluorescent protein (GFP) coupled by an internal ribosomal entry site (IRES) sequence. HEK293 cells were transiently transfected with the pdiTRPM4b/pdiTRPM5 vector using previously described methods and successfully transfected cells were visually identified by their green fluorescence in the patch clamp set up (Nilius *et al.* 2003). To evaluate the mechanisms of decavanadate (DV) action, we constructed a chimera in which the TRPM4 C-terminus was exchanged by the TRPM5 C-terminus. The rationale behind this is that we did not observe ATP effects on TRPM5 (N. D. Ullrich *et al.* unpublished observations). The chimera was obtained using the standard PCR overlap extension technique (Ho *et al.* 1989) with the human TrpM4 cDNA and the mouse TrpM5 cDNA as the templates; both constructed in the pCAGGSM2/IresGFP. The C-terminal part of TrpM4 cDNA (from aa G^{1047}) was replaced by the corresponding sequence of the TrpM5 cDNA (from aa Q^{981} until stop codon). The replacement sequence was created by standard PCR overlap extension (Ho *et al.* 1989). We used the following primers: on TrpM4 cDNA, forward primer; gacggcggacccagccg and reverse primer; ***gcaccacctg***gaatgtgtaactgaacatggc: and on TrpM5 cDNA forward primer; ***cagttacacattc***caggtggtgcaaggcaatgc and reverse primer; cggcttcggccagtaacg (overlapping sequences are in bold italic). The chimerical overlap PCR fragments were replaced into pCAGGSM2/TrpM4/IresGFP using *Asc* I and *Cla* I restriction enzymes. The sequence of the chimera was verified by sequence analysis. For evaluation of a putative DV binding site, we deleted the N-terminal or the C-terminal stretch in TRPM4 (^{332}RDRIRR, ^{1136}RARDKR). Deletions were constructed by the same overlap technique (Ho *et al.* 1989). Identical clusters of positive charges are not present in TRPM5. These sites resemble part of a putative ATP binding site in ABC ATPases comprising a stretch FSRDRK (Clausen *et al.* 2003).

Solutions

The extracellular solution for cell-attached measurements and the pipette solution for inside-out patch clamp measurements contained (mM): 156 NaCl, 5 $CaCl_2$, 1 $MgCl_2$, 10 glucose, 10 Hepes, buffered at pH 7.4 with NaOH. Before patch excision, the extracellular bath solution was changed to an 'internal solution' for inside-out patch clamp measurements, which contained (mM): 156 NaCl or KCl, 1 $MgCl_2$, 10 Hepes, 5 EGTA. The Ca^{2+} concentration of this solution was adjusted between 100 nM and 1000 μM by adding appropriate amounts of $CaCl_2$, as calculated by the CaBuf program (ftp://ftp.cc.kuleuven.ac.be/pub/droogmans/cabuf.zip). The pH of all solutions was adjusted to 7.2 with NaOH. In all inside-out studies, internal solutions were ATP free. All experiments were performed at room temperature (22–25°C).

Decavanadate was prepared as described in detail elsewhere (Csanady & Adam-Vizi, 2004). DV was applied from a stock solution of 50 mM Na_3VO_4 at pH 2.0, because DV is the major vanadium species at this pH. This stock solution was stored at +4°C and used within 24 h and was diluted into the bath just before each experiment (< 60 min). In all applications, we took care to only use solutions with a faint yellow colour, which is indicative of the presence of vanadate in the decamer form.

Electrophysiology

Currents were monitored in the inside-out patch clamp configuration with an EPC-9 (HEKA Elektronik,

Lambrecht, Germany). Patch electrodes had a DC resistance between 2 and 4 MΩ. An Ag–AgCl wire was used as a reference electrode. Sampling interval was 500 μs and filter setting was 1 kHz. In most of the experiments, we applied step protocols from a holding potential of 0 mV consisting of 500 ms steps to −100 mV followed by a 250 ms step to +100 mV. The interval between the pulses was 2 s. Patches were excised in the internal pipette solution at various intracellular Ca^{2+} concentrations. The first data point during a time course experiment was obtained within 2 s after excision, which corresponds to the stimulation interval. All DV experiments were done in symmetrical Na^{+}-containing solutions.

Data analysis

Electrophysiological data were analysed using WinASCD software (ftp://ftp.cc.kuleuven.ac.be/pub/droogmans/winascd.zip). Origin 7.0 (OriginLab, Northampton, MA, USA) was used to fit dose–response curves and the kinetic model described below. Significance was tested by the two sample Student's t test ($P < 0.05$ for significance). Pooled data are given as means ± S.E.M. of n cells.

Results

Desensitization of TRPM4 channels in inside-out patches

Figure 1*A* shows continuous recordings of TRPM4 currents in inside-out patches in response to repetitive voltage steps to −100 and +100 mV, immediately after patch excision in three different Ca^{2+} concentrations. Current amplitudes at all three Ca^{2+} concentrations decline with time after patch excision (Fig. 1*A*, left panel): the rate and extent of 'desensitization' are inversely related to the Ca^{2+} concentration applied to the inside of the patch. Interestingly, the current declines faster and to a larger extent at negative than at positive potentials. From the overlay of the currents at −100 and +100 mV (Fig. 1*A*, right panel) it can be appreciated that the kinetics of

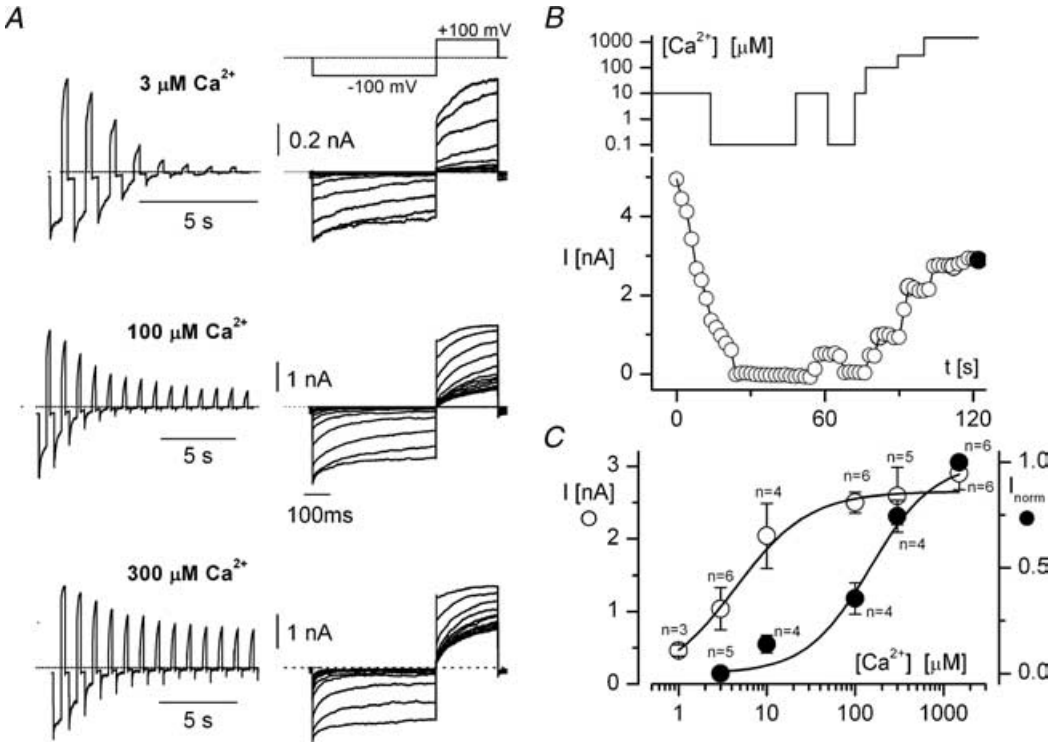

Figure 1. Desensitization of TRPM4 in inside-out patches
A, time course of current decline during repetitively applied voltage steps to −100 and +100 mV from a holding potential of 0 mV at Ca^{2+} concentrations of, respectively, 3 μM (top), 100 μM (middle) and 300 μM (bottom). Note the faster decline of inward currents than outward currents. *B*, time course of the changes in TRPM4 current following patch excision, and application of various Ca^{2+} concentrations after it has reached stationary levels. Current amplitudes at +100 mV at the Ca^{2+} concentrations indicated in the upper panel. Same voltage protocol as in Fig. 1*A*. *C*, dependence of the current amplitude immediately after patch excision and that at the steady-state level on Ca^{2+} concentration. Note the pronounced increase of EC_{50} at the steady-state level compared with that immediately after patch excision. Steady-state values were normalized to data in 1500 μM Ca^{2+} (filled circle in *B*). Data for the initial peak and the steady-state values were obtained form the same cells (see also supplementary data).

current activation immediately after patch excision is faster than at the stationary level, and that $[Ca^{2+}]$ has profound effects on current amplitude and activation rate. Also note that the currents at 3 μM Ca^{2+} are smaller than those at 100 and 300 μM Ca^{2+}, as expected for a Ca^{2+}-activated channel. Typically, these time courses scatter substantially (see supplementary information).

The current decay after patch excision might reflect a decline of the affinity of the TRPM4 channel for Ca^{2+}, which would explain the faster and more complete current reduction at low $[Ca^{2+}]$ compared with that at high $[Ca^{2+}]$. We therefore evaluated the Ca^{2+} concentration for half-maximal current activation (EC_{50}) immediately after patch excision and also after the currents reached a stationary level. Figure 1*B* shows the time course of the current decline at +100 mV in a medium with 10 μM Ca^{2+}. After the current has reached a stationary level, the inside-out patch is exposed to different Ca^{2+} concentrations. Figure 1*C* shows the average amplitudes of the current immediately after patch excision as a function of the Ca^{2+} concentration (open circles). The large error bars are indicative of the pronounced variability between cells. From the fit of the data points with $I = I_{max}/(1 + EC_{50}/[Ca^{2+}])$ we obtained an EC_{50} of 4.4 μM. Figure 1*C* also displays the stationary current amplitudes as a function of the Ca^{2+} concentration (filled circles). These values are normalized to the current amplitude at 1.5 mM Ca^{2+} obtained from the same patch and are therefore less sensitive to cell variability, hence the smaller error bars. We obtained an EC_{50} of 140 μM, which is at least 30 times larger than the value immediately after patch excision (for a more detailed discussion see supplementary data). These findings are consistent with a gradual decrease of the Ca^{2+} affinity of the channel following patch excision, which might be explained by a gradual loss of an intracellular regulator, and may partly explain the highly variable Ca^{2+} sensitivity between cells. It is worthwhile to mention that all EC_{50} values very much depend on the state of desensitization, the metabolic state of the cells, the normalization of the data and voltage protocol (slow decay at positive, fast decay at negative potentials).

A kinetic model for the Ca^{2+}-activated and voltage-dependent TRPM4 channel

Since a quantitative analysis of TRPM4 currents in excised patches is not feasible immediately after patch excision due to the rapid current decay, we have limited our analysis to the late phase, when the currents have reached a 'quasi' stationary level. Figure 2*A* shows current traces from a single patch at different Ca^{2+} concentrations during voltage steps ranging from −100 to +180 mV (increment 40 mV) applied from a holding potential of 0 mV. In Fig. 2*B* and *C*, we summarize the pooled data from several patches representing the voltage dependence of the initial value of the tail current recorded at −100 mV and the time constants of current relaxation. The current amplitudes were normalized to their asymptotic value at the highest Ca^{2+} concentration. From these data we conclude that higher cytoplasmic Ca^{2+} concentrations lead to larger current amplitudes, a slight leftward shift of the voltage-dependent activation curves and faster time constants for current activation at positive potentials.

To describe these data more quantitatively, we used a minimal kinetic model to describe the Ca^{2+}- and voltage-dependent gating of TRPM4. Given that voltage by itself is insufficient for channel activation in the absence of Ca^{2+}, we used a sequential model in which binding of Ca^{2+} precedes voltage-dependent channel activation, i.e.

$$C \underset{k_{-1}}{\overset{k_1 Ca}{\rightleftharpoons}} C^* \underset{\beta(V)}{\overset{\alpha(V)}{\rightleftharpoons}} O$$

C and C* represent the Ca^{2+}-free and Ca^{2+}-bound closed state of the channel, O its open state. $\alpha(V)$ increases and $\beta(V)$ decreases exponentially with voltage V. Ca^{2+} binding ($K_d = k_{-1}/k_1$) is assumed to be much faster than voltage-dependent gating. The steady-state channel open probability P_O and time constant τ of (de)activation for this model are given by:

$$P_O = \frac{\alpha'}{\alpha' + \beta} \quad \text{and} \quad \tau = \frac{1}{\alpha' + \beta}$$
$$\text{with } \alpha' = \frac{\alpha}{1 + K_d/[Ca^{2+}]} \qquad (1)$$

This model is compatible with the observed run-down of the channel after patch excision, as described above, since an increase of K_d will reduce P_O and increase τ. It also predicts that the open probability approaches unity at high Ca^{2+} concentrations and strong positive potentials, which justifies equating the normalized current amplitudes in Fig. 2*B* with open probabilities. A global fit of these equations to the experimental data of Fig. 2*B* and *C*, represented by the continuous lines, yielded the following parameters: $K_d = 87$ μM, $\alpha(V) = 0.0057 \exp(0.0060\, V)$ and $\beta(V) = 0.033 \exp(-0.019\, V)$. The dashed line represents simulated P_O values at the end of the 400 ms voltage pulse in 10 μM Ca^{2+}. This line fits these experimental data better than the steady-state P_O, as the steady state, especially at high positive voltages, is not fully reached at the end of the voltage steps.

The current traces in Fig. 2*D* simulated with the fitted parameters, assuming an ohmic open channel conductance and a reversal potential of 0 mV, resemble closely the experimental traces shown in Fig. 2*A*. Currents were calculated by:

$$I(V,t) = g\, P_O(t)\, V$$
$$P_O(t) = (P_O(\infty) - P_O(0))\,(1 - e^{-t/\tau}) + P_O(0) \qquad (2)$$

where P_O and τ were obtained from eqn (1), $P_O(\infty)$, $P_O(0)$ refer to steady-state and initial P_O values, respectively. Again, due to this variable desensitization in different individual cells and cell batches, the estimation of the K_D values scatter substantially (see supplementary data).

Modulation of TRPM4 by decavanadate

We have reported previously that ATP in its free form (ATP^{4-}) is a potent blocker of TRPM4 (Nilius *et al.* 2004). The vanadate decamer decavanadate (DV) has been widely used as a tool to interact with ATP binding, and ATP block of a non-selective Ca^{2+}-activated cation channel in brain capillary endothelium was recently shown to be antagonized by DV (Csanady & Adam-Vizi, 2004). We have therefore extended our study to the effects of DV on TRPM4 currents. Figure 3 illustrates the effects of 10 μM DV on TRPM4 currents when applied to the intracellular side of the patch. DV, which was applied after TRPM4 currents had reached a stationary level, induced a fast and fully reversible increase of inward current (Fig. 3*A*). Except for a small reduction at high DV concentrations (not in all cells) it had only minor effects on outward current (Fig. 3*A*). DV exerted pronounced effects on current kinetics (Fig. 3*B*): the typical current deactivation at negative and current activation at positive potentials was virtually abolished in the presence of 10 μM DV, indicating that DV strongly affects the gating of TRPM4 channels ($n > 20$ cells).

To quantify these effects of DV, we have measured the inward current amplitudes (I_{DV}) at −100 mV at different DV concentrations (Fig. 3*B* and *C*), and calculated the fractional current increase as $(I_{DV} - I_{control})/I_{control}$ at each concentration. The maximal current increase was 2.5-fold, with an EC_{50} of 1.9 μM and a Hill coefficient (n_H) of 1.8 (Fig. 3*C*). These effects of DV contrast with those of ATP^{4-}, which inhibited outward currents with an EC_{50} of 1.7 μM (Nilius *et al.* 2004).

Effect of decavanadate on the instantaneous current–voltage relation of TRPM4

The pronounced effect of DV on inward current amplitude and the lack of significant effect on the steady-state outward current amplitude could, in theory, be due to a DV-induced inward rectification of the TRPM4

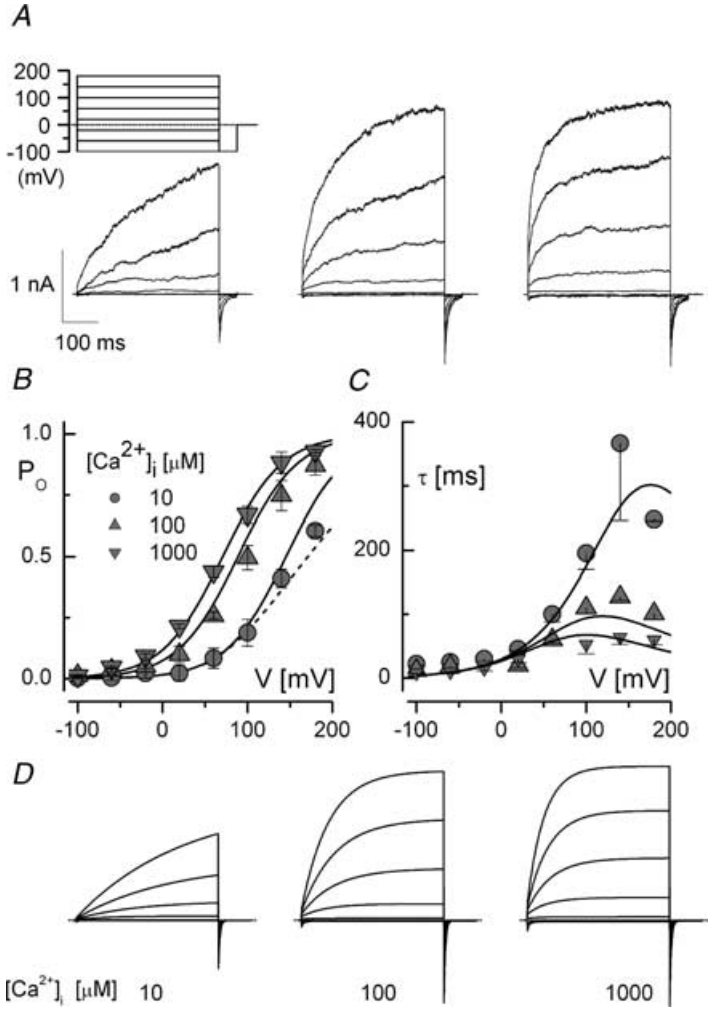

Figure 2. Quantitative analysis of the Ca^{2+} and voltage-dependence of TRPM4 currents
A, current traces at 10 μM (left), 100 μM (middle) and 1000 μM (right) Ca^{2+} recorded during voltage steps ranging from −100 to +180 mV (increment = 40 mV) from a holding potential of 0 mV, and followed by a short step to −100 mV. Note the increased current amplitude and faster kinetics at higher Ca^{2+} concentrations. *B*, initial tail current amplitudes during the step to −100 mV. These current amplitudes were normalized to the asymptotic value at high Ca^{2+} concentration and strong positive potentials. The continuous lines represent the fit of the steady-state probability predicted by the model (see text) to the experimental data; the dashed line is the predicted open probability at the end of the 400 ms step in 10 μM Ca^{2+} (pooled data from 4 cells). *C*, time constants of current activation as a function of membrane voltage at the 3 different Ca^{2+} concentrations. The continuous lines represent the fit of the time constants predicted by the model to the experimental data ($n = 4$). *D*, simulated current traces using the parameters from the global fit of the data in panels *B* and *C*.

channel. We have therefore evaluated the instantaneous current–voltage relation at negative potentials, using the protocol shown in Fig. 4*A*. After a pre-pulse to +100 mV, the membrane was clamped back to various negative potentials and the current immediately after stepping back to these potentials was determined. This protocol was applied to an inside-out patch either in the absence or in the presence of 10 μM DV. From the current–voltage relation (Fig. 4*B*) it can be seen that DV does not enhance the instantaneous current amplitude at any potential. It is therefore unlikely that the enhanced inward current in the presence of DV is due to a DV-induced inward rectification of TRPM4. The small reduction of the current amplitude at negative potentials may be due to the same blocking action of DV that reduces current amplitudes at positive potentials.

Effect of decavanadate on the voltage dependence of P_O

Both the enhanced inward current and the apparent lack of gating are consistent with a substantial slowing down of channel closure due to shift of the voltage dependence of $\beta(V)$ to more negative potentials. This would result in an increased open probability, especially at negative voltages. To confirm this, we have applied a classical tail current protocol to assess the fraction of open channels at various voltages. In order to cover an as wide as possible voltage range, we have measured the instantaneous amplitude of tail currents at −160 mV (Fig. 4*C*). These tail currents deactivate rapidly and almost completely in the absence of DV, but more slowly and incomplete in the presence of DV. The tail current amplitudes were converted to P_O, i.e. normalized to the asymptotic current amplitude in the same patch at high [Ca^{2+}] and strong positive potentials in the absence/presence of DV. The result of such an analysis is shown in Fig. 4*D* (pooled data from 6 cells). Assuming that DV does not affect K_d, we can deduce $\beta(V)/\alpha(V)$ from the fit of these normalized data with eqn (1). We obtained $\beta(V)/\alpha(V) = 4.4\exp(-0.032\,V)$ in the absence of DV compared with $\beta(V)/\alpha(V) = 0.12\exp(-0.0048\,V)$ in the presence of 10 μM DV. Because the tail currents in the presence of DV are much slower than under control conditions, the change in $\beta(V)/\alpha(V)$ is probably due to a change in $\beta(V)$ rather than $\alpha(V)$. Assuming that the effect of DV is entirely due to an effect on

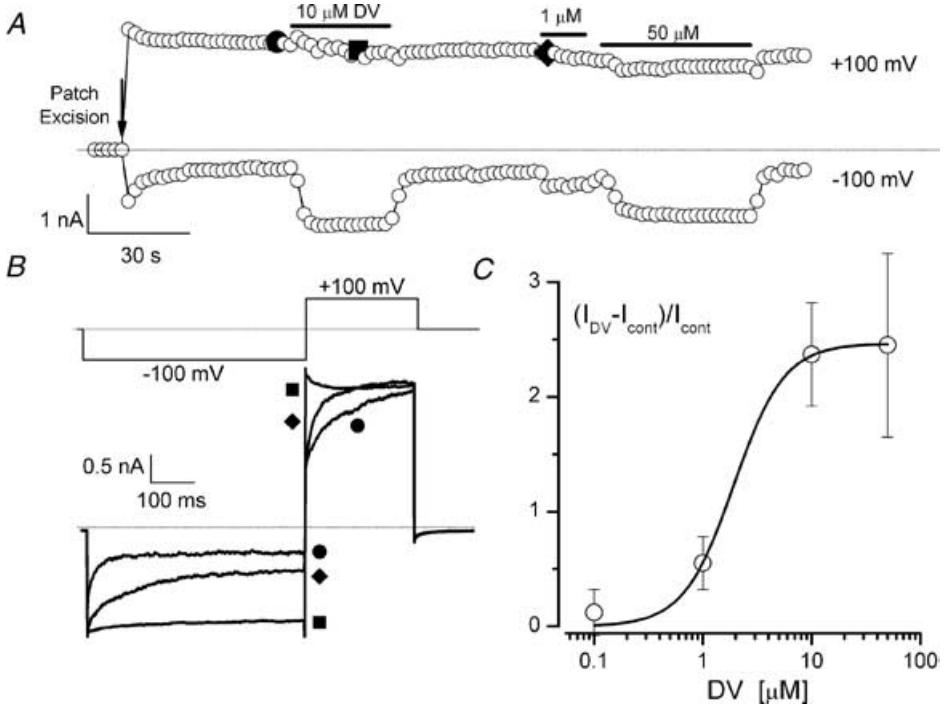

Figure 3. Modulation of TRPM4 by decavanadate in inside-out patches
A, time course of channel activity in an inside-out patch (same protocol as in Fig. 1*A*, excision in 1000 μM Ca^{2+} to delay current decay at +100 mV). Application of different concentrations of DV increases the inward current at −100 mV but not at +100 mV. *B,* current traces from the same experiment corresponding to the filled symbols in panel *A*, illustrating the effect of 1 and 10 μM DV on the kinetics of the current at −100 and +100 mV. Note the prominent increase of inward current in the presence of DV and the nearly step-like time course of the current (●, control; ■, 10 μM DV; ♦, 1 μM DV). *C,* concentration–response curve for the DV-induced increase of inward current at −100 mV defined as $(I_{DV} - I_{cont})/I_{cont}$, where I_{DV} and I_{cont} represent the current amplitudes in the present and absence of DV. The continous line represents a fit for a Hill equation with an EC_{50} of 1.9 μM and a slope n_H of 1.8 (data from 6 cells).

$\beta(V)$, simulated current traces ($\alpha(V)$ was taken from the controls, Fig. 2) recapitulate the experimental traces remarkably well (Fig. 4*C*, right panel).

Effects of decavanadate on the block of TRPM4 by ATP

Although the action of DV is clearly distinct from that of ATP, it cannot be excluded that DV affects the ATP block by some competitive action at ATP binding sites. We have therefore compared the concentration dependence of ATP block in the absence and presence of 5 μM DV. Figure 5*A* shows an example of the currents activated by 300 μM Ca^{2+} in the presence of DV, and subsequent block by different concentrations of ATP. Application of 8 μM free ATP^{4-} (corrected for the applied Ca^{2+} concentration of 300 μM) resulted in a fast and nearly complete block of the current (Fig. 5*A*), which was completely reversible (data not shown). Figure 5*B* shows some representative current traces in the presence of various ATP^{4-} concentrations that were used to evaluate the concentration dependence of the block. Figure 5*C* shows the fraction of unblocked current at +100 and −100 mV in the presence of various concentrations of ATP^{4-}. The block by ATP^{4-} could be described by:

$$\frac{I_{ATP}}{I_{control}} = \frac{1}{1 + [ATP^{4-}]/IC_{50}} \quad (3)$$

where IC_{50} represents the concentration of half-maximal block, which amounts to 130 nM. When compared with data in the absence of DV (Fig. 5*C*), DV sensitizes the block of TRPM4 by ATP approximately 10 times (compare also Nilius *et al.* 2004). Note that the block by ATP^{4-} in the presence of DV is voltage independent, as illustrated by overlap of the dose–response curves at −100 and +100 mV (Fig. 5*C*). It is therefore unlikely that the observed DV effects are linked to a competitive action of DV with the blocking ATP binding site.

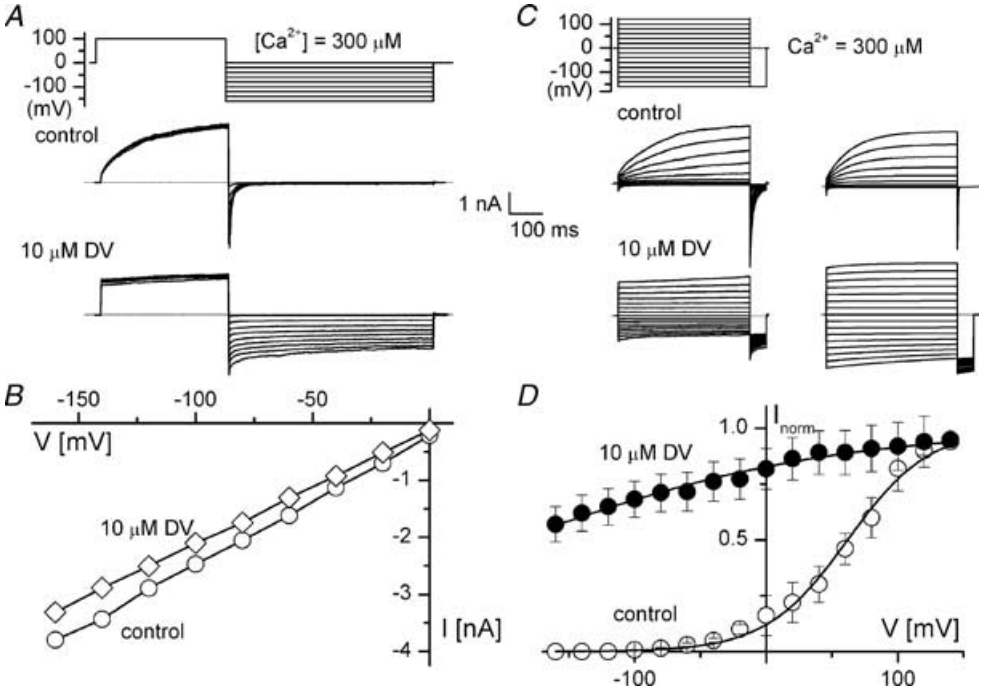

Figure 4. Effect of decavanadate on the instantaneous current–voltage relation of TRPM4 and on the voltage dependence of open probability of TRPM4
A, current traces during the voltage protocol shown at the top in the absence (middle) and the presence of 10 μM DV (bottom). Currents were activated by a depolarizing step to +100 mV, followed by 300 ms steps to voltages ranging from 0 to 160 mV (20 mV decrement). Holding potential is 0 mV, inside-out patch with 300 μM Ca^{2+}. *B, I–V* plots of the instantaneous amplitude of the tail currents shown in *A,* in the absence (○) and presence (◊) of 10 μM DV. *C,* current traces elicited by 400 ms pulses to potentials ranging from −160 to +140 mV and a subsequent 50 ms step to −160 mV. Note that the deactivation of the inward currents during the step to −160 mV is complete in the absence but not in the presence of 10 μM DV. The patch was exposed to 300 μM Ca^{2+}. *D,* voltage dependence of the normalized initial tail current amplitudes from 6 cells in the absence and presence of 10 μM DV. The continuous lines represent the open probabilities predicted by the kinetic scheme, assuming that K_d is not affected by DV. The fitted parameters for $\beta(V)/\alpha(V)$ were 4.4 exp(−0.032 *V*) under control conditions and 0.12 exp(−0.0048 *V*) in the presence of 10 μM DV. The right panel in *C* shows current traces simulated with these fitted parameters assuming that DV acts exclusively on $\beta(V)$.

The decavanadate effect requires the C-terminus of TRPM4

Preliminary experiments have shown that ATP does not block TRPM5 channels (N. D. Ullrich *et al.* unpublished observations). This finding has prompted us to test the effects of DV on TRPM5. Surprisingly, DV, applied under the same conditions as for TRPM4, has no effect on TRPM5 currents (Fig. 6). Panel *A* shows the typical increase of the inward current in TRPM4 immediately after application of DV. The traces on the right show the dramatic increase in current amplitude at negative potentials and the very slow kinetics of the current. Typically for TRPM4 is that a 'quasi' stationary current level is reached after patch excision. In contrast, TRPM5 shows a rapid and complete desensitization (Fig. 6*B*). However, application of DV did not delay this decay and did not detectably increase the current amplitude at negative potentials. Because the C-terminus of TRPM4 but not that of TRPM5 contains a putative ATP binding site resembling part of the nucleotide (decavanadate) binding site in SERCA, we have constructed a chimeric protein by exchanging the C-termini between both channels (TRPM4_CM5). As shown in Fig. 6*C*, the TRPM4 channel containing the C-terminus of TRPM5 shows a complete desensitization similar to that of TRPM5, which was not affected by DV. These data are summarized in Fig. 6*D*, showing current amplitudes before and 6 s (three sweeps) after application of DV at −100 and +100 mV. The dramatic increase of the current at −100 mV as observed for wild type TRPM4 was absent in both TRPM5 and TRPM4_CM5. The effects at +100 mV were not significant. Obviously, the C-terminus of TRPM4 is required for the action of DV.

Since DV contains six negative charges, which induce strong electrostatic interactions with sites accumulating positive charges and may form ATP binding sites as in various ABC ATPases, e.g. SERCA pumps (Csermely *et al.* 1985; Toyoshima *et al.* 2000; Clausen *et al.* 2003) and myosin (Pezza *et al.* 2002), we have searched for a similar motif in TRPM4. A cluster of positive charges is present in the C-terminus of TRPM4, similar to the FSRDRK motif in SERCA which has been found in TRPM4 as ^{1136}RARDKR. A similar motif is also present in the N-terminus of TRPM4, ^{332}RDRIRR. Deletion of the C-terminal stretch resulted in two dramatic changes: (1) desensitization was accelerated and (2) DV effects disappeared. Figure 7 shows these results. In the presence and absence of DV, TRPM4 activity decayed due to desensitization as described above (Fig. 7*A* and *B*). Deletion of the putative binding site resulted in a more rapid decay, indicating a much faster desensitization. However, DV effects could be detected

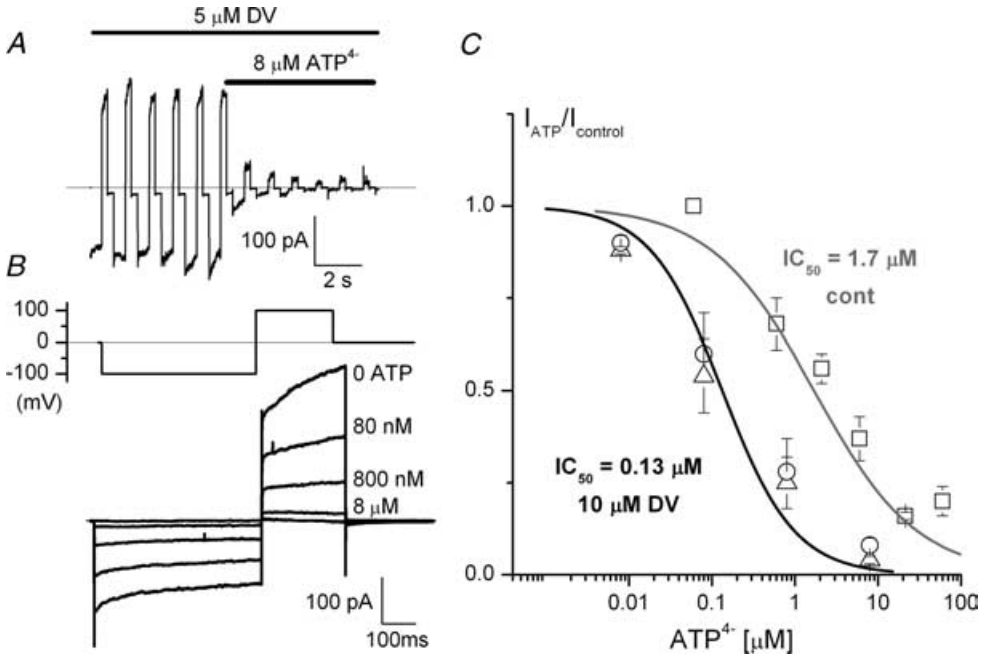

Figure 5. Effect of DV on the block of TRPM4 by ATP
A, time course of the effect of 8 μM free ATP^{4-} on TRPM4 currents in an inside-out patch (300 μM Ca^{2+}) in the presence of 5 μM DV. *B,* effect of various ATP^{4-} concentrations on the currents evoked by voltage steps to −100 and +100 mV in the presence of 5 μM DV and 300 μM Ca^{2+}. *C,* concentration dependence of the ATP block at −100 (Δ) and +100 mV (○) in the presence of 5 μM DV (pooled data from 5 cells). Current amplitudes were normalized to the maximal values +100 mV in the absence of ATP. The IC_{50} value for current inhibition at +100 mV was 0.13 μM. Note that the inhibition at −100 and +100 mV is not significantly different. □, control data obtained at +100 mV and in the absence of DV (compare also Nilius *et al.* 2004).

(Fig. 7*C* and *D*). Pooled data show a dramatic difference between wild type TRPM4 currents and R/K deletion mutants. The time constant of decay was significantly smaller in the R/K mutant than in wild type TRPM4 at +100 and −100 mV (Fig. 7*F*). As shown already above, desensitization occurred faster at −100 than at +100 mV. However, the decay in the presence DV was slower then in the control experiments. Figure 7*G* shows the analysis of the stationary values at 300 μM $[Ca^{2+}]_i$. For TRPM4, currents at −100 mV nearly completely disappear in the absence of DV, but in the presence of DV significantly larger inward currents remain. However, DV did not significantly affect the stationary value at +100 mV. For the R/K mutant, currents decay completely independent of the presence or absence of DV. Deletion of the N-terminal stretch, ^{332}RDRIRR, resulted in significantly reduced currents (mean value at 1500 μM and +100 mV was 2.8 ± 0.4 nA, $n = 6$ for wild type TRPM4, 143 ± 55 pA for the N-terminal R/K mutant). However, DV clearly increased the current at negative potentials (Fig. 7*G*). The relative increase of the current by 10 μM DV at 1500 μM Ca^{2+} was 2.6 ± 1.0 ($n = 5$) for −100 mV (same calculation as in Figs 3 and 6). These data are not significantly different from wild type TRPM4 (Fig. 3, 1000 μM $[Ca^{2+}]_i$). All these data together strongly indicate that the site of action of DV resides in the C-terminus of TRPM4.

Discussion

The Ca^{2+}-activated non-selective cation channel TRPM4 represents a molecular candidate for a large number of functionally similar Ca^{2+}-activated cation channels found in native cells types (see Introduction). Typical fingerprints of this channel are its activation by Ca^{2+}, its intrinsic voltage dependence and potent block by ATP^{4-} (Launay *et al.* 2002; Nilius *et al.* 2003, 2004). We present here a sequential kinetic model in which Ca^{2+} binding precedes voltage-dependent gating, which is able to describe the observed Ca^{2+}- and voltage-dependent gating behaviour of TRPM4 in inside-out patches. The analysis of channel activity in whole-cell experiments is hampered by a fast decay and mostly complete decay of the current (Nilius *et al.* 2003). Also in cell-free patches a fast current decay occurs immediately after patch excision, which levels off

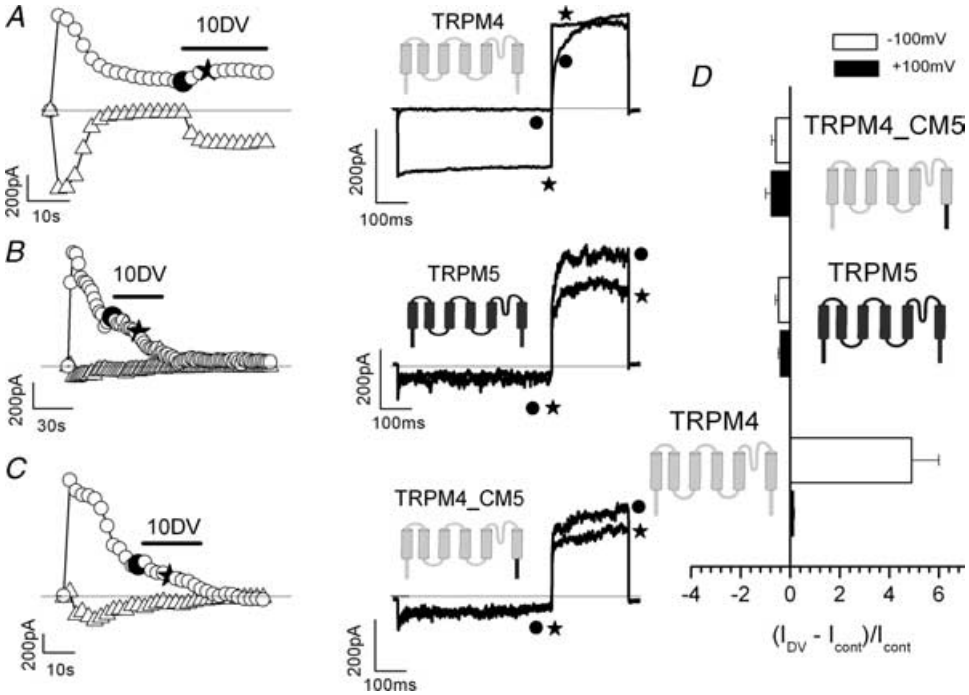

Figure 6. Differential effects of DV on wild type TRPM4 and TRPM5 and on a C-terminal TRPM4–TRPM5 chimera (TRPM4_CM5)

A, time course of channel activity in an inside-out patch of a wild type TRPM4-expressing cell (same protocol as in Fig. 1*A*, excision in 300 μM Ca^{2+}, time courses at +100 and −100 mV are shown). At the indicated time, 10 μM DV was added to the inner side of the patch. Note again the fast current increase at negative potentials. Superimposed traces before and during DV application are shown at the right (●, before DV; ★, during DV). *B*, DV application to an excised patch of a TRPM5-expressing cell. Same protocol as in *A*. Note the lack of DV action and the typical complete decay after patch excision. *C*, same protocol as in *A*, but from a cell expressing a chimeric channel of TRPM4 containing the C-terminus of TRPM5. *D*, pooled data from at least 4 cells (excised in 300 μM $[Ca^{2+}]_i$). The relative change of the current was measured 6 s (3 sweeps) after DV application. Data were obtained at −100 (open bars) and +100 mV (filled bars). Negative values indicate a decrease in current amplitude (desensitization). Note the dramatic difference at −100 mV between TRPM5 and the chimera, and TRPM4.

to a variable Ca^{2+}-dependent rest activity. Measured from the same cells, the EC_{50} after current decay is much larger than the value immediately after patch excision, indicative of a decline of the Ca^{2+} affinity of the TRPM4 channel immediately after patch excision. The slower current decay at higher Ca^{2+} concentrations is compatible with this contention, because a much larger shift of the Ca^{2+} activation curve is required to significantly reduce the open probability. Interestingly, a similar desensitization of non-selective Ca^{2+}-activated cation channels (NSC) has been observed in inside-out excised patches from pancreatic acinar cells (Maruyama & Petersen, 1984) and brain capillary endothelium (Csanady & Adam-Vizi, 2003). The rate of activation at positive potentials and the deactivation at negative potentials also declines during this desensitization phase, which is compatible with

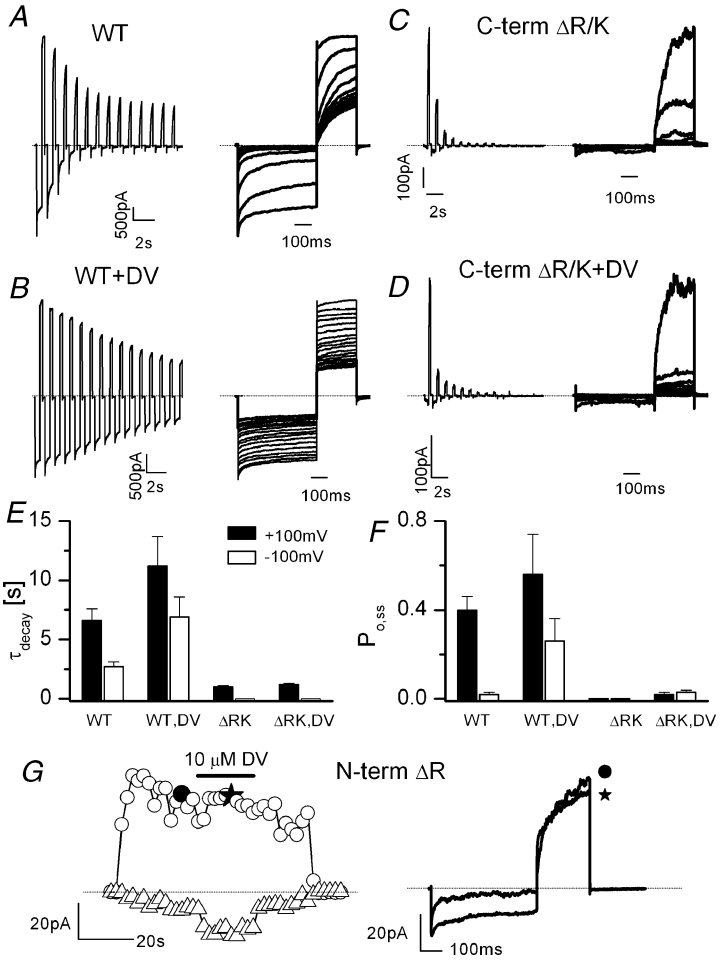

Figure 7. Differential effects of DV on wild type TRPM4 and a deletion mutant of a positively charged site in the C-terminus and N-terminus, C-term ΔR/K and N-term ΔR

A, time course of wild type TRPM4 activation after application of 300 μM $[Ca^{2+}]_i$ (same protocol as in Fig. 1*A*, superimposed traces are shown to the right of the time course, no application of DV). *B,* same protocol as in *A*; however, the patch was excised in 300 μM $[Ca^{2+}]_i$ and 10 μM DV. Note the changed kinetics of the currents. Decay (desensitization) is still present. *C,* same protocol as in *A* but now for the R/K deletion mutant (300 μM $[Ca^{2+}]_i$). Note the very fast decay but the lack of DV effects. *D,* same protocol as in *B*. The patch was excised in 10 μM DV. No apparent changes compared with *C*. *E,* pooled parameters of the mono-exponential fit (τ_{decay}) of time courses after patch excision from at least 4 cells. The decay at −100 mV is faster than at +100 mV ($P < 0.05$). In the presence of DV TRPM4 still desensitizes. Values at +100 mV are not significantly different; however, DV delays the decay at −100 mV as compared with data in the absence of DV ($P < 0.05$). The R/K mutant (ΔRK) showed a dramatically accelerated decay. *F,* 'steady state' values ($P_{o,ss}$) for currents after patch excision in 300 μM Ca^{2+}. The apparent steady state open probability at −100 (open bars) and +100 mV (filled bars) was calculated from the ratio of the current at the end of the measurement and the initial current immediately after excision. Note that the decay is much more complete in wild type TRPM4 at −100 mV, both in the absence of DV and the continuous presence of 10 μM DV (all $P < 0.05$). The R/K mutants desensitize completely. *G,* time course of activation of N-terminal R/K mutant after application of 1500 μM $[Ca^{2+}]_i$ (○, +100 mV; Δ, −100 mV). As indicated, 10 μM DV was applied. At the right, superimposed traces are shown before (●) and during (★) application of DV. Note the increase in the inward currents which is almost identical to the wild types TRPM4.

our model. The reason for desensitization is not yet understood, but it is likely that it will involve dephosphorylation processes or the loss of sensitizing cytosolic factors such as calmodulin. Ca^{2+} sensitivity of TRPM4 is very probably regulated. Desensitization might obviously also be the source for the scattering of the measured EC_{50} values for activation of TRPM4 by Ca^{2+} (compare also previously published values ranging from the submicromolar values to values exceeding 100 μM; Launay *et al.* 2002; Hofmann *et al.* 2003; Nilius *et al.* 2004). Even in our own studies, EC_{50} values measured in excised patches are scattered between 140 μM (this study) and 370 μM (Nilius *et al.* 2004). We describe here in detail that protocols for the measurement of the EC_{50} values for Ca^{2+} are hampered by desensitization (see supplementary data). Therefore, EC_{50} values for channels showing fast desensitization must be considered with caution. Some other reasons, which also apply for studies on TRPM5 showing the same kind of desensitization, can be understood from our quantitative approach. We describe here for the first time the interdependence of Ca^{2+} and voltage. The EC_{50} measurement results by definition from an estimation of $P_O/P_{O,max}$ (see supplementary data). Therefore, the measured EC_{50} depends on both the 'real' K_d value and on voltage. Changes in voltage dependence inevitably lead to changes in the EC_{50}. As usual, measurements of EC_{50} values are performed after desensitization has reached a 'steady state'. However, this steady-state level is variable even at the same Ca^{2+} concentration. A further reason for the scatter is an often overlooked methodological problem: Since it is very difficult to obtain the correct $P_{O,max}$ experimentally (in this case at high Ca^{2+} concentrations and very positive potentials), and the determination of EC_{50} strongly depends on the value of $P_{O,max}$ used for normalization, this can contribute to the scattering in inside-out experiments.

Our linear three-state kinetic scheme used for the description of dependence of P_O and of τ of (de)activation of the TRPM4 currents on $[Ca^{2+}]$ and voltage during the stationary phase after patch excision was also used to characterize the effects of decavanadate, a compound that competes with ATP at ATP-binding sites, as described for ATP-dependent transport proteins, especially for SERCA Ca^{2+} pumps (Csermely *et al.* 1985; Hua *et al.* 2000; Toyoshima *et al.* 2000). It has also been described that DV increases single channel conductance of NSCs (Popp & Gögelein, 1992; Csanady & Adam-Vizi, 2003) and is an activator of NSC channels in endothelium by antagonizing the ATP block (Csanady & Adam-Vizi, 2004). Here we show that DV modulates channel activity of TRPM4 heterologously expressed in HEK 293 cells, mainly by interfering with channel gating. From our analysis we conclude that the most likely effect of DV is a dramatic shift of the voltage dependence of channel closing ($\beta(V)$) towards negative potentials, resulting in a strongly reduced voltage -dependence of P_O in the investigated voltage range. As a consequence, robust inward currents occur at negative potentials, and the time-dependent components of the current during voltage step are small. This activation occurs in the micromolar range, and is not due to a substantial change in Ca^{2+} affinity of the channel. A similar effect of decavanadate has been recently described for NSCs in brain capillary endothelium (Csanady & Adam-Vizi, 2004), and was explained by a slowed channel closure caused by a high-affinity binding of DV to the open conformation of the channel (EC_{50} of 90 nM). In this same paper, Csanady & Adam-Vizi (2004) described an antagonistic effect of DV on the ATP block of these channels. They explained this ATP block by a high-affinity binding of ATP in the closed channel conformation, but competitively at the same site as DV. These effects of DV on ATP block are at variance with our present observation in TRPM4 channels, showing that DV actually sensitized ATP block and decreased the IC_{50} by a factor of 10. It is difficult to reconcile these data with a model whereby ATP and DV preferentially bind to the same site in the open and closed channel configuration, respectively. We assume that DV binds to a site, which interacts with the voltage-sensing mechanism (channel closing). The question remains how DV acts on TRPM4. Although it has been suggested that DV may act via lipid peroxidation of the membrane (Soares *et al.* 2003; Tiago *et al.* 2004), we think that this explanation is unlikely because of the very fast onset and the fast and complete reversibility of DV effects on TRPM4.

The unexpected finding that ATP blocks both inward and outward currents in the presence of DV suggests that the ATP block might be voltage independent, which is in contrast with our previous contention that ATP would act as an open pore blocker in the absence of DV. Our results therefore suggest that DV binds to a site, which modulates the voltage dependence of the channel rather than interfering with the blocking site of ATP^{4-}.

To evaluate the mechanisms of DV action, we have first tested whether the closely related channel TRPM5 responds to DV. TRPM5 was insensitive to ATP^{4-} at concentrations as high as 1 mM (N. D. Ullrich *et al.* unpublished observations). It might therefore not be completely unexpected that DV did not affect TRPM5. DV has been successfully used to identify the ATP binding site in SERCA (Toyoshima *et al.* 2000). Such a binding site shows some clear plasticity and depends on a structural motif rather than on a specific peptide sequence (Clausen *et al.* 2003). Decavanadate binding in the SERCA Ca^{2+} ATPase occurs in a spatial structure to which the nucleotide binding domain N, the actuator domain A, and the phosphorylation domain P all contribute (Hua *et al.* 2000). A putative ATP binding site in ABC ATPases is composed of elements with the sequences TETAL, FSRDRK, KGAPE,

RCLALA (Clausen *et al.* 2003). Especially interesting are highly positively charged sites, which have also been identified in the head segment of myosin (called subfragment 1) and bind DV (Tiago *et al.* 2004). The intracellular domains of TRPM4 contain multiple regions with a high density of positively charged residues. One of these sites is located in the C-terminus of TRPM4 and confers a stretch of six amino acids with four positive and one negative charge (^{136}RARDKR, R/K mutant). Such a motif is lacking in TRPM5. We have therefore first constructed a chimera of TRPM4 containing the C-terminus of TRPM5. This chimera shows some properties of TRPM5, i.e. a complete and rapid desensitization after patch excision, but lacks any effect of DV. Likewise, the R/K mutant also showed a complete lack of DV effect. Interestingly, the R/K mutant and also the chimeras showed changes in desensitization. It can be speculated that these sites are important for regulation of the Ca^{2+} sensitivity of TRPM4 and may be also involved in ATP binding. However, such a possible binding is different from the blocking site, because the chimeric channels showed a similar block by ATP^{4-} as the wild type TRPM4 channels ($IC_{50} = 0.5\ \mu M$ ATP^{4-}, data not shown, $n = 3$ for three concentrations).

A similar motif was found in the N-terminus of TRPM4, namely ^{332}RDRIRR, which also comprises four positive charges and one negative charge. Deletions of these motifs resulted in functional channels, which could still be, in contrast to the C-terminal deletion, modulated by DV. All these data together suggest that the C-terminus of TRPM4 is crucially involved in regulation of gating, and is at least part of the DV acceptor that can dramatically modulate the kinetic behaviour of this channel. However, this C-terminal site is very probably different from the blocking site for ATP^{4-}.

In conclusion, we have identified DV as the first strong modulator of voltage-dependent gating in the Ca^{2+}-activated cation channel TRPM4. DV might represent a novel tool to modulate endogenous TRPM4-mediated NSCs and may provide a possible way to differentiate between TRPM4 and TRPM5, and may contribute to our understanding of TRPM4 gating. Finally, it is tempting to speculate that an endogenous molecule with properties similar to those of DV may act as a physiological ligand for TRPM4.

References

Clausen JD, McIntosh DB, Vilsen B, Woolley DG & Andersen JP (2003). Importance of conserved N-domain residues Thr441, Glu442, Lys515, Arg560, and Leu562 of sarcoplasmic reticulum Ca^{2+}-ATPase for MgATP binding and subsequent catalytic steps. Plasticity of the nucleotide-binding site. *J Biol Chem* **278**, 20245–20258.

Colquhoun D, Neher E, Reuter H & Stevens CF (1981). Inward current channels activated by intracellular Ca in cultured cardiac cells. *Nature* **294**, 752–754.

Csanady L & Adam-Vizi V (2003). Ca^{2+}- and voltage-dependent gating of Ca^{2+}- and ATP-sensitive cationic channels in brain capillary endothelium. *Biophys J* **85**, 313–327.

Csanady L & Adam-Vizi V (2004). Antagonistic regulation of native Ca^{2+}- and ATP-sensitive cation channels in brain capillaries by nucleotides and decavanadate. *J General Physiol* **123**, 743–757.

Csermely P, Varga S & Martonosi A (1985). Competition between decavanadate and fluorescein isothiocyanate on the Ca^{2+}-ATPase of sarcoplasmic reticulum. *Eur J Biochem* **150**, 455–460.

Egorov AV, Hamam BN, Fransen E, Hasselmo ME & Alonso AA (2002). Graded persistent activity in entorhinal cortex neurons. *Nature* **420**, 173–178.

Eto W, Hirano K, Hirano M, Nishimura J & Kanaide H (2003). Intracellular alkalinization induces Ca^{2+} influx via non-voltage-operated Ca^{2+} channels in rat aortic smooth muscle cells. *Cell Calcium* **34**, 477–484.

Guinamard R, Chatelier A, Lenfant J & Bois P (2004). Activation of the Ca^{2+}-activated nonselective cation channel by diacylglycerol analogues in rat cardiomyocytes. *J Cardiovasc Electrophysiol* **15**, 342–348.

Guinamard R, Rahmati M, Lenfant J & Bois P (2002). Characterization of a Ca^{2+}-activated nonselective cation channel during dedifferentiation of cultured rat ventricular cardiomyocytes. *J Membr Biol* **188**, 127–135.

Halonen J & Nedergaard J (2002). Adenosine 5′-monophosphate is a selective inhibitor of the brown adipocyte nonselective cation channel. *J Membr Biol* **188**, 183–197.

Ho SN, Hunt HD, Horton RM, Pullen JK & Pease LR (1989). Site-directed mutagenesis by overlap extension using the polymerase chain reaction. *Gene* **77**, 51–59.

Hofmann T, Chubanov V, Gudermann T & Montell C (2003). TRPM5 is a voltage-modulated and Ca^{2+}-activated monovalent selective cation channel. *Current Biol* **13**, 1153–1158.

Hua S, Inesi G & Toyoshima C (2000). Distinct topologies of mono- and decavanadate binding and photo-oxidative cleavage in the sarcoplasmic reticulum ATPase. *J Biol Chem* **275**, 30546–30550.

Hurwitz CG, Hu VY & Segal AS (2002). A mechanogated nonselective cation channel in proximal tubule that is ATP sensitive. *Am J Physiol* **283**, F93–104.

Koch J & Korbmacher C (1999). Osmotic shrinkage activates nonselective cation (NSC) channels in various cell types. *J Membr Biol* **168**, 131–139.

Koivisto A, Siemen D & Nedergaard J (2000). Norepinephrine-induced sustained inward current in brown fat cells: alpha(1)-mediated by nonselective cation channels. *Am J Physiol* **279**, E963–977.

Launay P, Fleig A, Perraud AL, Scharenberg AM, Penner R & Kinet JP (2002). TRPM4 is a Ca^{2+}-activated nonselective cation channel mediating cell membrane depolarization. *Cell* **109**, 397–407.

Liman ER (2003). Regulation by voltage and adenine nucleotides of a Ca^{2+}-activated cation channel from hamster vomeronasal sensory neurons. *J Physiol* **548**, 777–787.

Liu D & Liman ER (2003). Intracellular Ca^{2+} and the phospholipid PIP_2 regulate the taste transduction ion channel TRPM5. *Proc Natl Acad Sci U S A* **100**, 15160–15165.

Magistretti J & Alonso A (2002). Fine gating properties of channels responsible for persistent sodium current generation in entorhinal cortex neurons. *J General Physiol* **120**, 855–873.

Maruyama Y & Petersen OH (1982). Cholecystokinin activation of single-channel currents is mediated by internal messenger in pancreatic acinar cells. *Nature* **300**, 61–63.

Maruyama Y & Petersen OH (1984). Single calcium-dependent cation channels in mouse pancreatic acinar cells. *J Membr Biol* **81**, 83–87.

Miyoshi H, Yamaoka K, Garfield RE & Ohama K (2004). Identification of a non-selective cation channel current in myometrial cells isolated from pregnant rats. *Pflügers Arch* **447**, 457–464.

Nilius B, Prenen J, Droogmans G, Voets T, Vennekens R, Freichel M, Wissenbach U & Flockerzi V (2003). Voltage dependence of the Ca^{2+}-activated cation channel TRPM4. *J Biol Chem* **278**, 30813–30820.

Nilius B, Prenen J, Voets T & Droogmans G (2004). Intracellular nucleotides and polyamines inhibit the Ca^{2+}-activated cation channel TRPM4b. *Pflügers Arch* **448**, 70–75.

Perez CA, Huang L, Rong M, Kozak JA, Preuss AK, Zhang H, Max M & Margolskee RF (2002). A transient receptor potential channel expressed in taste receptor cells. *Nature Neurosci* **5**, 1169–1176.

Petersen OH (2002). Cation channels: homing in on the elusive CAN channels. *Current Biol* **12**, R520–522.

Pezza RJ, Villarreal MA, Montich GG & Argarana CE (2002). Vanadate inhibits the ATPase activity and DNA binding capability of bacterial MutS. A structural model for the vanadate–MutS interaction at the Walker A motif. *Nucl Acids Res* **30**, 4700–4708.

Popp R & Gögelein H (1992). A calcium and ATP sensitive nonselective cation channel in the antiluminal membrane of rat cerebral capillary endothelial cells. *Biochim Biophys Acta* **1108**, 59–66.

Ringer E, Russ U & Siemen D (2000). Beta(3)-adrenergic stimulation and insulin inhibition of non-selective cation channels in white adipocytes of the rat. *Biochim Biophys Acta* **1463**, 241–253.

Rodighiero S, De Simoni A & Formenti A (2004). The voltage-dependent nonselective cation current in human red blood cells studied by means of whole-cell and nystatin-perforated patch-clamp techniques. *Biochim Biophys Acta* **1660**, 164–170.

Simard JM & Chen M (2004). Regulation by sulfanylurea receptor type 1 of a non-selective cation channel involved in cytotoxic edema of reactive astrocytes. *J Neurosurg Anesthesiol* **16**, 98–99.

Soares SS, Aureliano M, Joaquim N & Coucelo JM (2003). Cadmium and vanadate oligomers effects on methaemoglobin reductase activity from Lusitanian toadfish: in vivo and in vitro studies. *J Inorg Biochem* **94**, 285–290.

Suh SH, Vennekens R, Manolopoulos VG, Freichel M, Schweig U, Prenen J, Flockerzi V, Droogmans G & Nilius B (1999). Characterisation of explanted endothelial cells from mouse aorta: electrophysiology and Ca^{2+} signalling. *Pflügers Arch* **438**, 612–620.

Suh SH, Watanabe H, Droogrnans G & Nilius B (2002). ATP and nitric oxide modulate a Ca^{2+} activated non-selective cation current in macrovascular endothelial cells. *Pflügers Arch* **444**, 438–445.

Tiago T, Aureliano M & Gutierrez-Merino C (2004). Decavanadate binding to a high affinity site near the myosin catalytic centre inhibits F-actin-stimulated myosin ATPase activity. *Biochem* **43**, 5551–5561.

Toyoshima C, Nakasako M, Nomura H & Ogawa H (2000). Crystal structure of the calcium pump of sarcoplasmic reticulum at 2.6 A resolution. *Nature* **405**, 647–655.

Wu SN (2003). Large-conductance Ca^{2+}-activated K^+ channels: physiological role and pharmacology. *Curr Med Chem* **10**, 649–661.

Zhainazarov AB (2003). Ca^{2+}-activated nonselective cation channels in rat neonatal atrial myocytes. *J Membr Biol* **193**, 91–98.

Acknowledgements

We are grateful to V. Flockerzi, R. Vennekens and U. Wissenbach (Homburg) for providing us the human TRPM4 clone and to R. F. Margolskee (Howard Hughes Medical Institute, Mount Sinai School of Medicine, New York) and C. A. Perez (Rockefeller University, New York) for the mouse TRPM5 DNA. We thank Dr L. Csanády (Budapest) for providing a preprint of a manuscript in press. We thank K. Talavera, Grzegorz Owsianik and Nina Ullrich (Leuven) for helpful discussions. This work was supported by the Belgian Federal Government, the Flemish Government, the Onderzoeksraad KU Leuven (GOA 2004/07, F.W.O. G.0214.99, F.W.O. G.0136.00, F.W.O. G.0172.03, Inter-university Poles of Attraction Program, Prime Ministers Office IUAP). T.V. is a postdoctoral fellow of the Fund for Scientific Research-Flanders (Belgium) (FWO-Vlaanderen).

Supplementary material

The online version of this paper can be accessed at: DOI: 10.1113/jphysiol.2004.070839
http://jp.physoc.org/cgi/content/full/jphysiol.2004.070839/DC1 and contains supplementary material entitled: Estimation of EC_{50} values in experiments with desensitizing channels.
This material can also be found at: http://www.blackwellpublishing.com/products/journals/suppamt/tjp/tjp524/tjp524sm.htm